Available online at www.sciencedirect.com

ScienceDirect

Ceramics International 35 (2009) 855–860

CERAMICS INTERNATIONAL

www.elsevier.com/locate/ceramint

Effects of $SrTiO_3$ additives on the structure and microwave dielectric properties of $Ba_{4.2}Sm_{9.2}Ti_{18}O_{54}$ ceramics

Jianhua Zhu, Wenzhong Lu *, Wen Lei, Shuai Wan

Department of Electronic Science and Technology, Huazhong University of Science and Technology, Wuhan, Hubei 430074, PR China

Received 7 November 2007; received in revised form 30 November 2007; accepted 6 March 2008
Available online 3 July 2008

Abstract

The effects of $SrTiO_3$ additives on the microstructure and the dielectric properties of $Ba_{4.2}Sm_{9.2}Ti_{18}O_{54}$ (BST) materials have been investigated. The microstructure of BST doped with $SrTiO_3$ was analyzed using X-ray diffraction (XRD), scanning electron microscopy (SEM) and electron probe microanalyzer (EPMA). The XRD, SEM and EPMA results showed that small amounts of $SrTiO_3$ (less than 4 wt.%) could be accommodated in BST while a secondary metatitanate phase appeared in the samples with 8 wt.% $SrTiO_3$ added, the addition of $SrTiO_3$ increased the lower solubility limit (x values) of $Ba_{6-3x}Sm_{8+2x}Ti_{18}O_{54}$. The relative permittivities and the TC_f values showed an approximately linear increase with increasing additions of $SrTiO_3$. It was observed that near zero TC_f values could be achieved with the addition of $SrTiO_3$ to BST ceramics. With 4 wt.% $SrTiO_3$ addition and sintered at 1360 °C for 2 h, BST ceramics exhibited excellent dielectric properties: $\varepsilon_r = 81.2$, $Q_f = 8470$ GHz and $TC_f = -1.5$ ppm/°C.

Keywords: C. Dielectric properties; Ceramics; Microstructure

1. Introduction

For over 30 years, dielectric ceramics based on BaO–Ln_2O_3–TiO_2 (where Ln are lanthanide elements) have been focused on because of their excellent microwave properties. A combination of a high-dielectric constant, low-dielectric loss and high-temperature stability of the permittivity makes them very important for the applications in microwave communication devices. The earliest work on these systems is credited to Bolton [1] and Kolar et al. [2]. The crystal structure of these ceramics belongs to the tungsten bronze structural family and consists of a three-dimensional framework of corner-sharing perovskite-like TiO_6 octahedra. Linked at the corners in a complex way they yield three types of openings: large pentagonal sites (A_2-sites), tetragonal sites (A_1-sites) and small triangular sites. The conventional formula $Ba_{6-3x}Ln_{8+2x}Ti_{18}O_{54}$ has been accepted for this system and the basic structural formula is $[A_1]_{10}[A_2]_4Ti_{18}O_{54}$ [3–5]. According to Ohsato [6] the lanthanide cations occupy the tetragonal channels, Ba^{2+} cations fill the pentagonal channels and the remaining Ba ions share the tetragonal channels with the lanthanides. The triangular channels are empty. The lower solubility limit (x) of $Ba_{6-3x}Sm_{8+2x}Ti_{18}O_{54}$ is 0.3 [7]. High permittivity of 78 and high $Q_f = 9720$ GHz have been reported when $x = 0.6$ and Ln = Sm [8]. However, this system has a high-negative TC_f of about -10 ppm/°C, thus a lot of work has been done to tune TC_f to near zero including partial substitution of Nd^{3+}/La^{3+} with Sm^{3+} in the rhombic channels [9,10]. Substitution of Sr^{2+} with Ba^{2+} has also been found to be very helpful in stabilizing the low-TC_f behavior [11–13], but the Q_f values decreased if a near zero TC_f value is needed. In the present study, $SrTiO_3$ ceramics have been used as additives in an effort to tune the TC_f of $Ba_{4.2}Sm_{9.2}Ti_{18}O_{54}$ (BST) ceramics to near zero. Unlike BST ceramics with a tungsten bronze structure, $SrTiO_3$ ceramics feature perovskite structure. Wise et al. [14] reported that the $SrTiO_3$ ceramics have permittivities of about 290 and high-positive TC_f values of about 1647 ppm/°C. Therefore, it is possible using $SrTiO_3$ as additives to improve the TC_f values of BST. In the present work, the effects of $SrTiO_3$ additives on the structural and microwave dielectric properties of BST have been investigated.

---

* Corresponding author. Tel.: +86 27 8754 2594; fax: +86 27 8754 3134.
E-mail address: lwz@mail.hust.edu.cn (W. Lu).

0272-8842/$34.00 © 2008 Elsevier Ltd and Techna Group S.r.l. All rights reserved.
doi:10.1016/j.ceramint.2008.03.015

2. Experimental procedures

Samples were prepared by the conventional solid-state reaction method. Reagent grade $BaCO_3$, Sm_2O_3, TiO_2 and $SrTiO_3$ with the purity of over 99.5 wt.% were used as raw materials. The starting materials were mixed according to the stoichiometries of $Ba_{4.2}Sm_{9.2}Ti_{18}O_{54}$ using deionised water and zirconia milling media. The mixtures were calcined at 1250 °C for 2 h. To form the mixed compositions, controlled amounts of $SrTiO_3$ were added to the calcined BST. The mixed powders were then remilled for 3 h and dried. Then the dried powders with PVA binders were pressed into disks 15 mm in diameter and 7–10 mm in thickness under a pressure of 100 MPa. Samples were sintered at 1340–1380 °C for 2 h in an air atmosphere. The bulk densities of the samples were measured by Archimedes' method. X-ray diffraction (XRD) experiments were performed on bulk samples using a Philips X'Pert PRO diffractometer operating at 40 kV, 40 mA with a fixed divergence slit of 0.9570°. A continuous scan was carried out using monochromatic Cu Kα radiation filtered through a Ni foil with 2θ angles in the range of 10–70° and a step size of 0.02°. The microstructure of the as-sintered surface was studied using field emission scanning electron microscope (FE-SEM) model FEI Sirion 200. The selected samples were ground on 1200 grade SiC paper, polished on diamond paste to 0.5 μm and thermally etched at 1260 °C for 10 min. The composition analyses of the thermally etched samples were performed by electron probe microanalyzer (EPMA) model JEOL JXA-8800R. The dielectric properties were measured using dielectric post-resonator technique developed by Hakki and Coleman [15]. The temperature coefficient of resonant frequency (TC_f) was also measured by the same method in the temperature range of 25–75 °C.

3. Results and discussion

The variation of bulk densities as a function of the addition of $SrTiO_3$ and sintered at temperatures between 1340 and 1380 °C for 2 h are shown in Fig. 1. The densities of the sintered ceramics were significantly affected by the addition amounts of $SrTiO_3$ and sintering temperatures. Addition of $SrTiO_3$ to BST ceramics causes a marked reduction in density. With the increasing addition amounts of $SrTiO_3$, the densities of the ceramics sintered at 1360 °C decreased from 5.71 g/cm^3 for pure BST to 5.56 g/cm^3 for the samples with the addition of

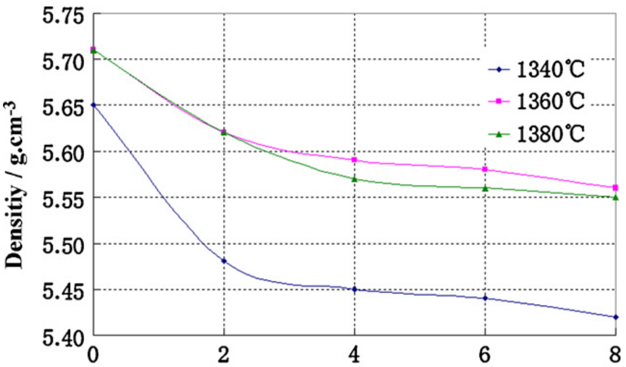

Fig. 1. The variation of bulk densities with amounts of $SrTiO_3$ added into BST sintered at different temperature for 2 h.

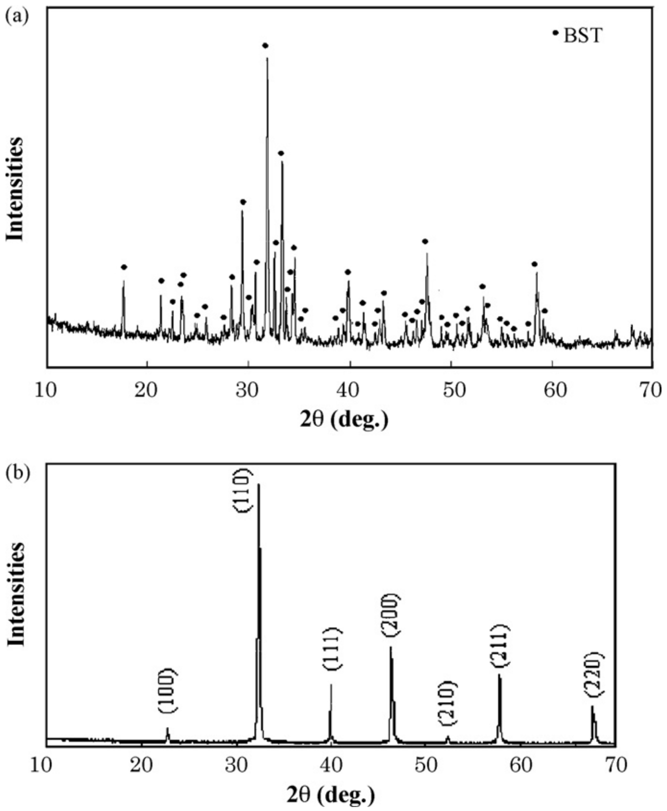

Fig. 2. XRD patterns of BST calcined at 1250 °C for 2 h and $SrTiO_3$ powder: (a) BST and (b) $SrTiO_3$.

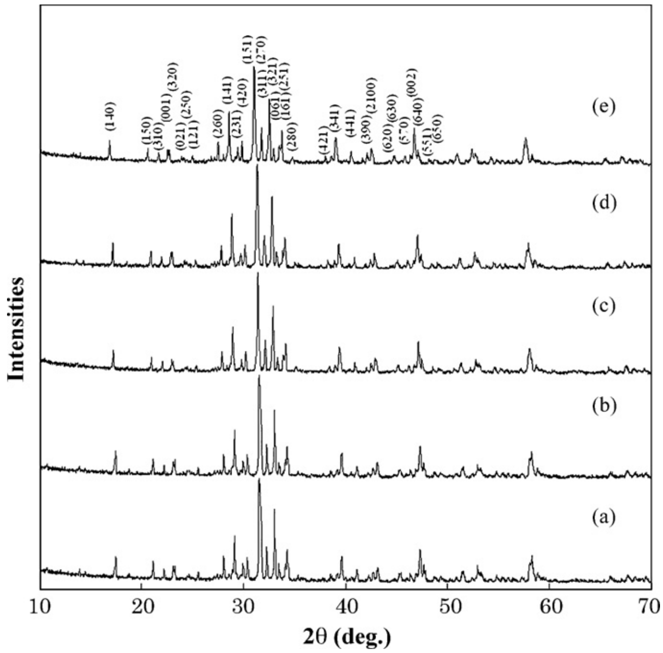

Fig. 3. XRD patterns of sintered BST ceramics with various addition amounts of $SrTiO_3$ and sintered at 1360 °C for 2 h where (a) 0 wt.%; (b) 2 wt.%; (c) 4 wt.%; (d) 6 wt.% and (e) 8 wt.%.

8 wt.% $SrTiO_3$. The ceramics sintered at 1360 °C have the highest densities.

Fig. 2 shows the X-ray diffraction patterns of (a) BST powder calcined at 1250 °C for 2 h and (b) $SrTiO_3$ powder. All the peaks in Fig. 2(a) can be assigned to that of the orthorhombic tungsten bronze type compounds, designated as $Ba_{6-3x}Sm_{8+2x}Ti_{18}O_{54}$ solid solutions [7]. In Fig. 2(b), all the peaks can be recognized as the $SrTiO_3$ single phase with perovskite structure (JCPDS 39-0487).

Fig. 3 shows the XRD patterns of BST ceramics with $SrTiO_3$ additives and sintered at 1360 °C. All the XRD patterns of Fig. 3(a)–(e) can be assigned to that of the orthorhombic tungsten bronze type compounds, designated as $Ba_{6-3x}Sm_{8+2x}Ti_{18}O_{54}$ solid solutions. With the increasing addition contents of perovskite-type $SrTiO_3$ on BST-based tungsten bronze structure, extra peaks were not observed even at the highest concentration of 8 wt.% $SrTiO_3$. It was considered that the possible reflections from a secondary phase might overlap with the tungsten bronze structure reflections. No significant changes in the XRD patterns were observed as reported by Silva et al. [16] and Zhu et al. [17] where small amounts (less than 10 wt.%) of similar perovskite-type $Li_2O–Nd_2O_3–4TiO_2$ and $NdAlO_3$ were added to BNT structure, respectively.

Typical scanning electron microscopy (SEM) micrographs of the as-sintered surfaces of BST ceramics with $SrTiO_3$ additives and sintered at different temperatures are shown in Fig. 4. The ceramics show typical columnar grain morphology usually observed in $Ba_{6-3x}Ln_{8+2x}Ti_{18}O_{54}$ (Ln = Nd and Sm) ceramics [16,17]. The SEM results confirm the occurrence of phases identified in the XRD patterns. It is noticeable that the size of the columnar grain increases with increasing $SrTiO_3$ content as well as sintering temperatures.

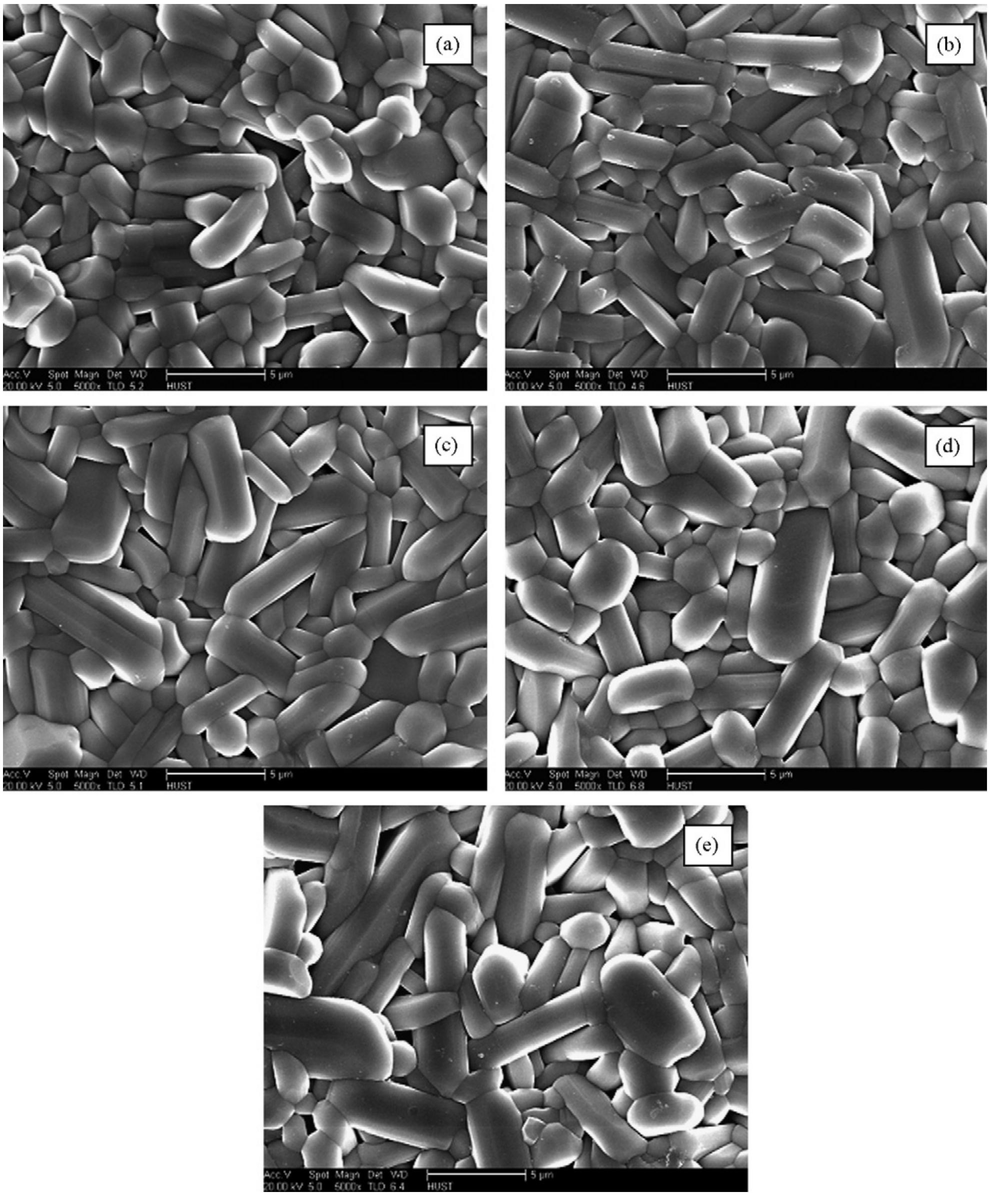

Fig. 4. FE-SEM micrographs of BST-based ceramics with various addition amounts of $SrTiO_3$ and sintered for 2 h where (a) 4 wt.%, 1340 °C; (b) 0 wt.%, 1360 °C; (c) 4 wt.%, 1360 °C; (d) 8 wt.%, 1360 °C and (e) 4 wt.%, 1380 °C.

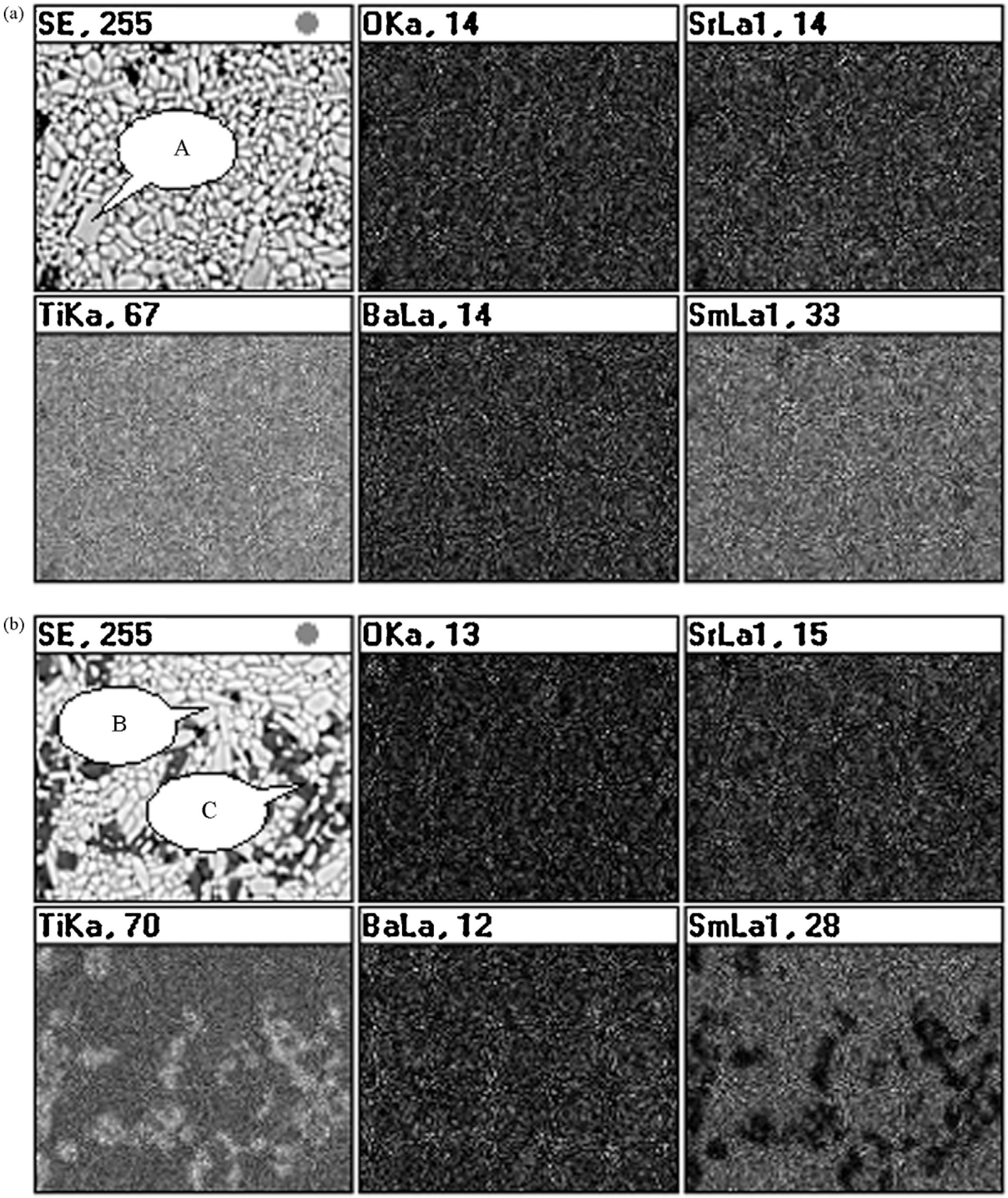

Fig. 5. EPMA surface scan patterns of BST doped with $SrTiO_3$ sintered at 1360 °C for 2 h where (a) 4 wt.% and (b) 8 wt.%.

No obvious second phases could be found with increasing addition contents of $SrTiO_3$. Furthermore, with increasing sintering temperature, significant grain growth was observed with accompanying reduction in porosity; therefore, samples sintered at 1360 °C displayed improved densification and the highest densities. For samples sintered at 1380 °C the microstructure exhibited abnormal growth of the grains resulting in density decrease.

Fig. 5 and Table 1 show the EPMA patterns of the polished samples. As a bright dot means high intensity of the element, we recognized each phase on the basis of the dot darkness. Fig. 5(a) shows a homogeneous phase and means that BST formed a solid solution with $SrTiO_3$, the Sr^{2+} occupied the A1 sites in tungsten bronze structure. Fig. 5(b) shows a mixed phases structure, where the bright matrix phase is BST:$SrTiO_3$ solid solution and the black secondary phase is barium–strontium–samarium metatitanate. It is probable that, as the concentration of $SrTiO_3$ increases, the lower solubility limit (x) of $Ba_{6-3x}Sm_{8+2x}Ti_{18}O_{54}$ is reached and a secondary metatitanate phase starts to form, as the phase diagram predicts. In this paper, the solid solution limit of $SrTiO_3$ in BST is thought to be about 4 wt.% and the resultant phase would correspond to

Table 1
The comparison of EPMA results among grain A, B and C in Fig. 5

	Ti K (at.%)	Sr L (at.%)	Ba L (at.%)	Sin L (at.%)	O (at.%)
Grain A	20.78	0.68	5.32	10.26	62.96
Grain B	21.33	1.71	4.43	9.50	63.04
Grain C	27.67	0.35	6.85	1.05	64.09

$Ba_{6-3x}Sm_{8+2x}Ti_{18}O_{54}$ with $x = 0.4$, the addition of $SrTiO_3$ increased the lower solubility limit (x) of $Ba_{6-3x}Sm_{8+2x}Ti_{18}O_{54}$.

Fig. 6 shows the microwave dielectric properties of BST ceramics with increasing additions of $SrTiO_3$ sintered at different temperatures for 2 h. Additions of $SrTiO_3$ increased the dielectric constant slightly and this observed change is attributed to the similar decrease of x values in $Ba_{6-3x}Sm_{8+2x}Ti_{18}O_{54}$ solid solutions, it had been reported [6] that the decrease of x values in $Ba_{6-3x}Sm_{8+2x}Ti_{18}O_{54}$ solid solutions would lead to the increase of dielectric constant and TC_f values. $SrTiO_3$ improved the permittivities of BST from 79.7 to 83.0 for samples with 8 wt.% additions and sintered at 1360 °C. As a function of sintering temperatures, the ceramics sintered at 1360 °C had the highest densities and therefore exhibited the highest permittivities. Fig. 6(b) shows the variation in Q_f values of BST ceramics with various additions of $SrTiO_3$. The entire range of compositions investigated exhibit a decrease in the Q_f values, the modest additions of 4 wt.% $SrTiO_3$ had virtually no effect on the Q_f values of BST, but further addition of $SrTiO_3$ led to a rapid decrease in the Q_f values, the existence of the second phase was thought to lead to the decrease. As a result of the poor densification, the samples sintered at 1340 °C exhibited the lowest Q_f values. Nevertheless, additions of $SrTiO_3$ are detrimental to the Q_f values of BST-based ceramics. Fig. 6(c) shows the change in TC_f values with different addition amounts of $SrTiO_3$ and sintering temperatures. In a similar way to the variation of permittivities, the TC_f values show an approximately linear increase with increasing content of the additives. $SrTiO_3$ improved the TC_f of BST from −10.8 to −1.5 ppm/°C when 4 wt.% $SrTiO_3$ was added. It is apparent that the TC_f values of tungsten bronze structured BST ceramics can be tuned to near zero with additions of perovskite structured $SrTiO_3$.

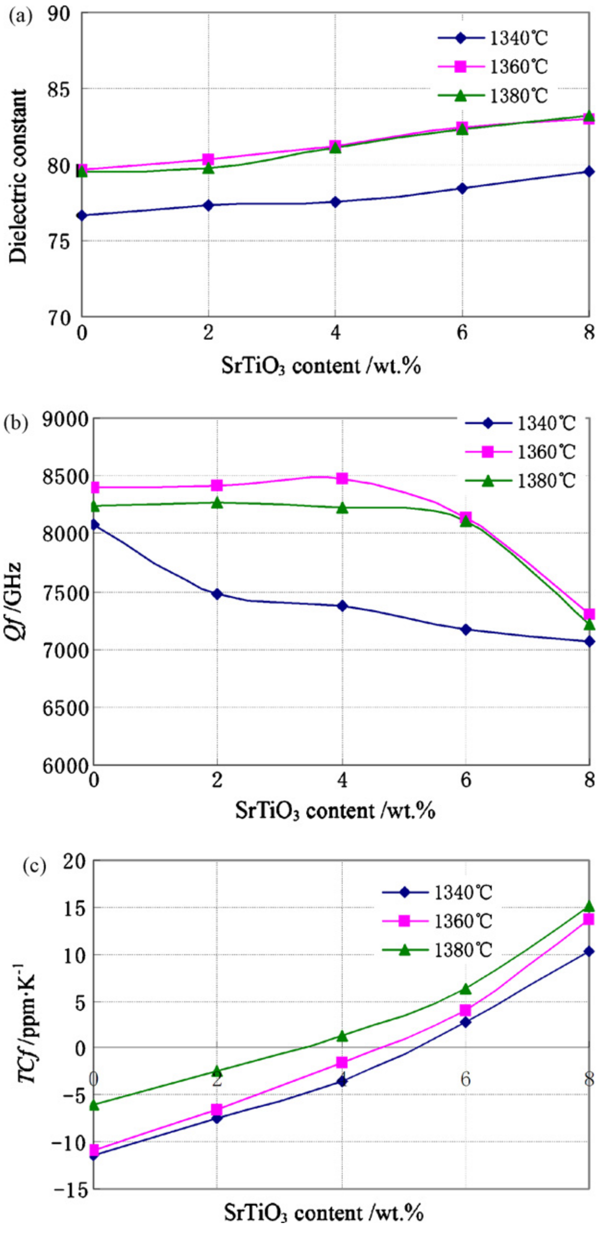

Fig. 6. Microwave dielectric properties of BST ceramics with various addition amounts of $SrTiO_3$ and sintered at different temperature for 2 h: (a) dielectric constant, (b) Q_f values, and (c) TC_f values.

4. Conclusions

The additions of $SrTiO_3$ decreased the densities of BST ceramics. Small additions of perovskite structure $SrTiO_3$ (less than 4 wt.%) could be accommodated in BST-based tungsten bronze structure, but EPMA results revealed a secondary metatitanate phase in BST-based ceramics with 8 wt.% $SrTiO_3$ added, the solid solution limit of $SrTiO_3$ in BST is thought to be about 4 wt.% and the resultant phase would corresponds to $Ba_{6-3x}Sm_{8+2x}Ti_{18}O_{54}$ with $x = 0.4$, therefore, the addition of $SrTiO_3$ increased the lower solubility limit (x) of $Ba_{6-3x}Sm_{8+2x}Ti_{18}O_{54}$. The relative permittivities and the TC_f values showed an approximately linear increase with increasing additions of $SrTiO_3$, which was attributed to the similar decrease of x values in $Ba_{6-3x}Sm_{8+2x}Ti_{18}O_{54}$ solid solutions. It was observed that near zero TC_f values could be achieved with the addition of $SrTiO_3$ additives to BST ceramics. The modest additions of less than 4 wt.% $SrTiO_3$ had no obviously effect on the Q_f values of BST-based ceramics, but further addition of $SrTiO_3$ led to a rapid decrease in the Q_f values. With 4 wt.% $SrTiO_3$ addition and sintered at 1360 °C for 2 h, BST ceramics exhibited excellent dielectric properties: $\varepsilon_r = 81.2$, $Q_f = 8470$ GHz and $TC_f = -1.5$ ppm/ °C.

References

[1] R.L. Bolton, Temperature compensating ceramic capacitors in the system baria–rare-earth oxide–titania, PhD Thesis, The University of Illinois, 1968.

[2] D. Kolar, Z. Stadler, S. Gaberscek, D. Suvorov, Ceramic dielectric properties of selected compositions in the BaO–TiO_2–Nd_2O_3 system, Ber. Dt. Keram. Ges. 55 (1978) 346–347.

[3] R. Ubic, I.M. Reaney, W.E. Lee, Microwave dielectric properties of solid-solution phase in system BaO–Ln_2O_3–TiO_2 (Ln = lanthanide cation), Int. Mater. Rev. 43 (5) (1998) 205–219.

[4] H. Ohsato, T. Ohhashi, H. Kato, S. Nishigaki, T. Okuda, Microwave dielectric properties and structure of the $Ba_{6-3x}Sm_{8+2x}Ti_{18}O_{54}$ solid solutions, Jpn. J. Appl. Phys. 34 (1) (1995) 187–191.

[5] T. Negas, P. Davies, Materials and processes for wireless communications, Ceram. Trans. 53 (1995) 179–196.

[6] H. Ohsato, Science of tungsten bronze-type like $Ba_{6-3x}R_{8+2x}Ti_{18}O_{54}$ (R = rare earth) microwave dielectric solid solutions, J. Eur. Ceram. Soc. 21 (2001) 2703–2711.

[7] H. Ohsato, T. Ohhashi, S. Nishigaki, T. Okuda, K. Sumiya, S. Suzuki, Formation of solid solution of new tungsten bronze-type microwave dielectric compounds $Ba_{6-3x}R_{8+2x}Ti_{18}O_{54}$ (R = Nd and Sm, $0 \leq x \leq 1$), Jpn. J. Appl. Phys. 32 (9B) (1993) 4323–4326.

[8] H. Ohsato, H. Kato, M. Mizuta, S. Nishigaki, T. Okuda, Microwave dielectric properties of the $Ba_{6-3x}(Sm_{1-y},R_y)_{8+2x}Ti_{18}O_{54}$ (R = Nd and La) solid solutions with zero temperature coefficient of the resonate frequency, Jpn. J. Appl. Phys. 34 (9B) (1995) 5413–5417.

[9] Y.J. Wu, X.M. Chen, Bismuth/samarium cosubstituted $Ba_{6-3x}Nd_{8+2x}$-$Ti_{18}O_{54}$ microwave dielectric ceramics, J. Am. Ceram. Soc. 83 (7) (2000) 1837–1839.

[10] N. Ichinose, H. Amada, Preparation and microwave dielectric properties of the BaO·$(Sm_{1-x}La_x)_2O_3$·5TiO_2 ceramic system, J. Eur. Ceram. Soc. 21 (2001) 2751.

[11] S. Nishigaki, H. Kato, S. Yano, R. Kamimura, Microwave dielectric properties of (Ba,Sr)O–Sm_2O_3–TiO_2 ceramics, Am. Ceram. Soc. Bull. 66 (9) (1987) 1405–1410.

[12] M. Imaeda, K. Ito, M. Mizuta, H. Ohsato, Microwave dielectric properties of $Ba_{6-3x}Sm_{8+2x}Ti_{18}O_{54}$ solid solutions with Sr substituted for Ba, Jpn. J. Appl. Phys. 36 (9B) (1997) 6012–6015.

[13] M. Suzuki, H. Ohsato, K. Kakimoto, T. Nagatomo, T. Otagiri, Crystal structure and microwave dielectric properties of $(Ba_{1-\alpha}Sr_\alpha)_{6-3x}Sm_{8+2x}$ $Ti_{18}O_{54}$ solid solutions, J. Eur. Ceram. Soc. 26 (2006) 2035–2038.

[14] P.L. Wise, I.M. Reaney, W.E. Lee, T.J. Price, D.M. Iddles, D.S. Cannell, Structure–microwave property relations in $(Sr_xCa_{(1-x)})_{n+1}Ti_nO_{3n+1}$, J. Eur. Ceram. Soc. 21 (2001) 1723–1726.

[15] B.W. Hakki, P.D. Coleman, A dielectric resonator method of measuring inductive capacitance in the millimetre range, IEEE Trans. Microw. Theory Tech. 8 (1960) 402–410.

[16] A. Silva, F. Azough, R. Freer, C. Leach, Microwave dielectric ceramics in the system BaO–Li_2O–Nd_2O_3–TiO_2, J. Eur. Ceram. Soc. 20 (2000) 2727–2734.

[17] J.H. Zhu, E.R. Kipkoech, W.Z. Lu, Effects of $LnAlO_3$ (Ln = La, Nd and Sm) additives on the properties of $Ba_{4.2}Nd_{9.2}Ti_{18}O_{54}$ ceramics, J. Eur. Ceram. Soc. 26 (2006) 2027–2030.